On the Potential of Phase-change Adsorbents for CO2 Capture by Temperature Swing Adsorption

Author(s):
Joss, Lisa; Hefti, Max; Bjelobrk, Zoran; Mazzotti, Marco

Publication date:
2017-07

Permanent link:
https://doi.org/10.3929/ethz-b-000233993

Originally published in:
Energy Procedia 114, https://doi.org/10.1016/j.egypro.2017.03.1375

Available online at www.sciencedirect.com

ScienceDirect

Energy Procedia 114 (2017) 2271 – 2278

Energy Procedia

13th International Conference on Greenhouse Gas Control Technologies, GHGT-13, 14-18 November 2016, Lausanne, Switzerland

On the potential of phase-change adsorbents for CO_2 capture by temperature swing adsorption

Lisa Joss[b†], Max Hefti[a], Zoran Bjelobrk[a], Marco Mazzotti[a]*

[a]*Institute of Process Engineering, ETH Zurich, Sonneggstr. 3, 8092 Zurich, Switzerland*

Abstract

The objective of this work is to assess the potential of a novel class of metal organic framework (MOF) materials recently introduced [McDonald et al., Nature, 2015, 519, 303] for post-combustion CO_2 capture by temperature swing adsorption (TSA). In particular, we present figures for the process performance obtained from optimizing operating conditions of a four-step TSA cycle. Our results show that high purity and high recovery can be attained. Subsequently, we benchmark the performance in terms of energy consumption and productivity to a state-of-the-art TSA process using zeolite 13X [Joss. et al. Chem. Eng. Sci. under review]. While the energy consumption is similar, a higher productivity can be obtained using these MOF materials. Finally, we make a comparison to amine-scrubbing processes and show that, after applying heat integration, similar performance can be expected.

Peer-review under responsibility of the organizing committee of GHGT-13.

Keywords: CO_2 capture; TSA; MOF; mathematical modelling; optimization

1. Introduction

In recent years, a variety of alternative processes to amine scrubbing have been investigated with regard to their potential in post-combustion CO_2 capture applications. Solid sorbents and the corresponding adsorption-based separation processes have received significant attention due to their stability and non-volatility of the sorbent.

* Corresponding author. Tel.: +41 632 2456; fax: +41 632 1141.
E-mail address: marco.mazzotti@ipe.mavt.ethz.ch
† Current address: Imperial College London, South Kensington Campus, SW7 2AZ London, United Kingdom

Peer-review under responsibility of the organizing committee of GHGT-13.
doi:10.1016/j.egypro.2017.03.1375

Nomenclature

e_{dry}	thermal energy penalty of the drying step (MJ/kg_{CO2})
e_{TSA}	thermal energy penalty of the TSA unit (MJ/kg_{CO2})
e_{tot}	total thermal energy penalty of the TSA process (MJ/kg_{CO2})
e_{w_P}	energy penalty of the drying unit per mass water (MJ/kg_{H2O})
$N^P_{CO_2}$	Amount of CO_2 produced during one cycle (mol)
$N^P_{N_2}$	Amount of N_2 in the CO_2 product (mol)
$N^F_{CO_2}$	Amount of CO_2 fed to the process during one cycle (mol)
$N^F_{N_2}$	Amount of N_2 fed to the process during one cycle (mol)
Pr	productivity of the TSA process ($kg_{CO2}/(m^3h)$)
r	CO_2 recovery (–)
Φ	CO_2 purity (–)

Tailoring materials towards optimal properties for post-combustion CO_2 capture is a challenge that is being addressed by numerous researchers. In particular, metal-organic-frameworks (MOFs) is considered to be a class of materials able to revolutionize separations due to the high degree of flexibility and control in pore size and surface chemistry. Numerous materials with promising properties have been synthesized and characterized, e.g. Mg-MOF-74 with unprecedented high CO_2 uptake capacities [1], or materials that undergo structural changes depending on the partial pressure of CO_2 [2]. Considerable interest in the community was provoked by a recent contribution by McDonald et al [3], who presented six diamine-appended MOFs (mmen-M_2(dobpdc), where M is the metal center) that behave as phase-change materials without exhibiting the disadvantages typical of other phase change adsorbents, i.e., hysteresis and changes in volume. In the following, the materials mmen-M_2(dobpdc) will be abbreviated as MOF-M, where M is the corresponding metal center.

These materials exhibit step-shaped CO_2 adsorption isotherms due to a unique cooperative insertion of CO_2 into the framework at and above a characteristic temperature dependent step pressure. In addition, they appear to show a high CO_2/N_2 selectivity and an affinity for CO_2 that is hardly affected by the presence of water vapor, hence, they represent attractive candidate materials for adsorption-based CO_2 capture.

This proceeding summarizes some major findings reported in our previous work [4], where a quantitative assessment of these materials' performance for post-combustion capture by a temperature swing adsorption (TSA) process was carried out for the first time.

2. Methodology

2.1. Isotherm model

Model-based design of adsorption processes requires an accurate model of the adsorption equilibrium that describes the adsorbed phase concentration as a function of composition, pressure and temperature. A continuously differentiable function is necessary in order to avoid numerical issues, hence the use of a weighted-dual site Langmuir isotherm, as suggested by Hefti et al. [4]. In this work, N_2 adsorption is assumed to be negligible. This assumption is justified by the data available in the literature [5].

The rationale behind the w-DSL isotherm is that there exists a partial pressure at which the material undergoes a phase transition, and the adsorption behavior on the material sites below and above that partial pressure can be described by two different dual site Langmuir isotherms, $n_L(p,T)$ and $n_U(p,T)$, respectively.

$$n(p,T) = n_{\mathrm{L}}(p,T)(1 - w(p,T)) + n_{\mathrm{U}}(p,T)w(p,T) \tag{1}$$

$$n_{\mathrm{L}} = \frac{n_{\mathrm{L}}^{\infty}\, b_{\mathrm{L}} p}{1 + b_{\mathrm{L}} p} \tag{2}$$

$$n_{\mathrm{U}} = \frac{n_{\mathrm{U}}^{\infty} b_{\mathrm{U}} p}{1 + b_{\mathrm{U}} p} + b_{\mathrm{H}} p \tag{3}$$

$$b_{\alpha} = b_{\alpha}^{\infty} \exp\left(\frac{E_{\alpha}}{RT}\right); \quad \alpha = \mathrm{L}, \mathrm{U}, \mathrm{H} \tag{4}$$

The transition is accounted for by a log-logistic weighting function, $w(p,T)$, that is centered in $p_{\mathrm{step}}(T)$ and has a width $\sigma(T)$.

$$w(p,T) = \left(\frac{\exp\left(\frac{\ln(p)-\ln(p_{\mathrm{step}}(T))}{\sigma(T)}\right)}{1+\exp\left(\frac{\ln(p)-\ln(p_{\mathrm{step}}(T))}{\sigma(T)}\right)}\right)^{\gamma} \tag{5}$$

$$p_{\mathrm{step}}(T) = p_{\mathrm{step},0} \exp\left(\frac{-H_{\mathrm{step}}}{R}\left(\frac{1}{T_0} - \frac{1}{T}\right)\right) \tag{6}$$

$$\sigma(T) = \chi_1 \exp\left(\chi_2\left(\frac{1}{T_0} - \frac{1}{T}\right)\right) \tag{7}$$

The parameters of the w-DSL isotherm were estimated by fitting eq. (1) to the measured adsorption isotherms provided by McDonald et al. [3]. The non-linear chi-square test function was minimized using the non-linear optimization algorithm fminsearchbnd implemented in Matlab. The parameters were estimated sequentially, i.e., those parameters describing the adsorption before the step (n_{L}^{∞}, b_{L}^{∞}, E_{L}^{∞}) were estimated first, and then kept constant for the estimation of the remaining parameters. Parameter uncertainty is reported as the 90% confidence interval calculated according to Smith [6].

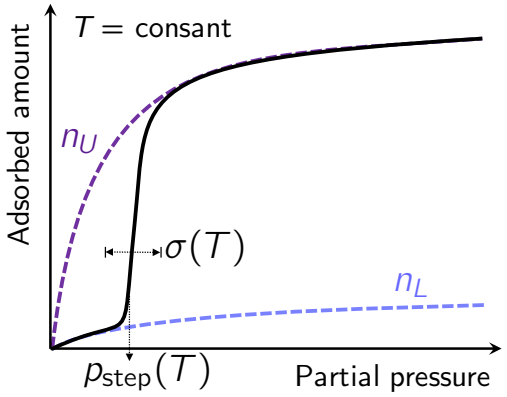

Fig. 1 Schematic representation of the weighted dual-site Langmuir (w-DSL) isotherm

2.2. TSA process

In this work, diamine-appended MOFs are assessed for their use in a TSA process aimed at capturing CO_2 from post-combustion flue gases. A flue gas whose composition is representative of a coal fired power plant is considered,

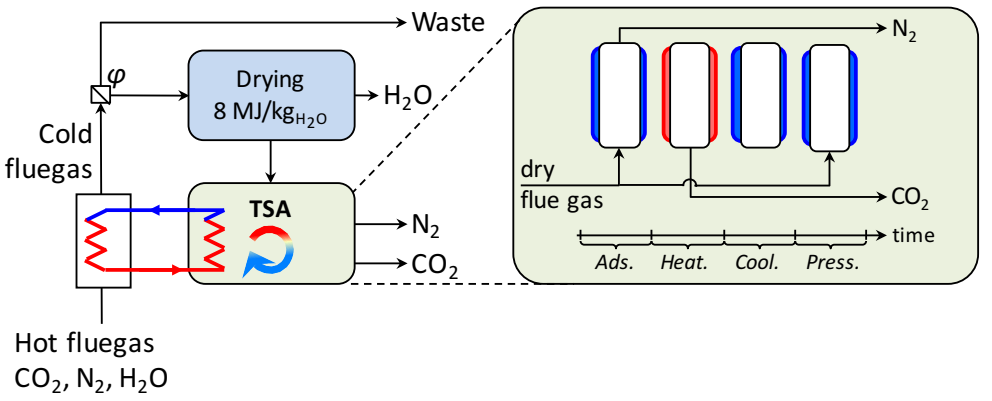

Fig. 2 Scheme of the considered TSA process (adapted from [4]). The water content contained in the flue gas is removed with a dedicated drying step prior to the TSA. Heat integration of the TSA unit with a low grade heat source (e.g. the hot flue gas) can be accounted for, as well as temperature equalization between heating and cooling steps.

i.e., a CO_2/N_2 stream (12:88 v/v on a dry basis) containing 4% water vapor. The design of TSA processes offers many degrees of freedom, such as the cycle configuration (sequence, direction and inter-connectivity of the individual steps), the column geometry and the operating conditions, i.e., the temperature of the heating and cooling fluids, the superficial velocity and the duration of the individual steps. The chosen column geometry is representative of a shell and tube reactor where the tubes are packed with adsorbent material and a heat transfer fluid is conveyed through the shell side. The temperature levels of the heating and cooling thermofluid are fixed to 420 K and 300 K, respectively, such as to be representative of available heat sources and sinks that allow for heat integration. A simple four step cycle that contains the most important features of TSA cycles while minimizing complexity (see Fig. 2) is considered. A drying step that removes water vapor completely precedes the TSA unit. The energetic penalty of the drying step is assumed to be equal to that of a silica guard which is regenerated at 150°C [7] and requires e_w = 8 MJ/kg$_{H2O}$.

2.3. Solution approach

The TSA process is simulated using a one-dimensional detailed model which was reported [8] and validated [9] in previous works. It consists of a system of partial differential algebraic equations describing mass, energy and momentum balances. The equations are discretized spatially and integrated in time for a single column with periodic boundary conditions reflecting the sequence of steps and boundary conditions. All model parameters are reported in Tables 1 and 2. The performance indicators are computed by integrating the inlet and outlet component and heat flows once a cyclic steady state (CSS) is reached. The chosen performance indicators are the CO_2 purity (Φ), CO_2 recovery (r), the productivity (Pr) and the specific energy consumption ($e_{tot} = e_{TSA} + e_{dry}$):

$$\Phi = \frac{N^P_{\mathrm{CO_2}}}{N^P_{\mathrm{CO_2}} + N^P_{\mathrm{N_2}}}, \qquad r = \frac{N^P_{\mathrm{CO_2}}}{N^F_{\mathrm{CO_2}}} \tag{8}$$

$$\mathrm{Pr} = \frac{N^P_{\mathrm{CO_2}}}{V_{\mathrm{bed}}\, t_{\mathrm{cycle}}}, \qquad e_{\mathrm{TSA}} = \frac{1}{N^P_{\mathrm{CO_2}}} \int_0^{t_{\mathrm{cycle}}} \max(0, \dot{Q}_{\mathrm{in}}), \qquad e_{\mathrm{dry}} = \frac{e_{\mathrm{w}} \varphi N^F_{\mathrm{H_2O}}}{N^P_{\mathrm{CO_2}}} \tag{9}$$

The performance of different materials is compared for optimal operation of the considered process: the operating conditions are optimized such as to maximize the productivity and minimize the specific energy consumption, while satisfying imposed constraints on the purity and recovery of the CO_2 product. The following optimization problem is solved:

$$\begin{aligned} \underset{\mathbf{x}}{\text{minimize}} \quad & (-\mathrm{Pr}, e_{\mathrm{tot}}) \\ \text{subject to} \quad & r \geq 0.90 \\ & \Phi \geq 0.96 \end{aligned} \tag{10}$$

Where $\mathbf{x} = \{t_{\mathrm{ads}}, t_{\mathrm{heat}}, t_{\mathrm{cool}}\}$ are the decision variables. A modified version of the multi-level coordinate search algorithm, which can handle multiple objectives and non-linear constraints [10] was employed to solve the optimization problem. The objectives and constraints are computed at each iteration by solving the TSA model.

Table 1. Model parameters. Two values are indicated ($\alpha_{\mathrm{MOF\text{-}Mn}}/\alpha_{\mathrm{MOF\text{-}Mn}}$) whenever a difference between MOF-Mn and MOF-Mg applies

Parameter	Value	Units
Column length	1.2	m
Column inner radius	15	mm
Column outer radius	16	mm
Heat capacity wall	4×10^6	J/(m^{3}K)
Heat capacity adsorbent	1600/1500	J/(kgK)
Heat transfer fluid/wall	100	W/(m^{2}K)
Heat transfer wall/bed	20	W/(m^{2}K)
Material density	3200	kg/m^3
Particle density	860	kg/m^3
Bed density	575	kg/m^3
Particle diameter	2	mm
CO_2 mass transfer coefficient	0.15	s^{-1}
Heat of adsorption	58.1/67.2	kJ/mol

3. Results

The focus is set on two materials out of those presented by McDonald et al. [3], i.e., the MOF-Mn and MOF-Mg. These were identified as the most promising materials because they exhibit a phase transition at very low CO_2 partial pressures, which is beneficial for the adsorption of CO_2 from low concentration sources [3].

3.1. Adsorption equilibria

Fig. 3 shows the CO_2 adsorption equilibrium measurements provided by McDonald et al. [3] together with the w-DSL fits for MOF-Mn and MOF-Mg. The fitted isotherm parameters are reported in Table 2. The confidence intervals of the parameters are rather large, because of some data points likely associated to a significant experimental error, particularly in the region near p_{step}, where the isotherms are very steep and hence difficult to measure. Overall, the proposed w-DSL model provides an accurate description of the experimental isotherms.

Table 2. Fitted isotherm parameters for MOF-Mn and MOF-Mg together with the 90% confidence intervals.

Parameter	MOF-Mn	MOF-Mg	Units
n_L^∞	0.138 ± 0.026	0.146 ± 0.068	mol/kg
b_L^∞	(6 ± 13)×10^{-6}	0.009 ± 0.091	bar^{-1}
E_L	44.8 ± 5.5	31 ± 26	kJ/mol
n_U^∞	2.629 ± 0.064	3.478 ± 0.064	mol/kg
b_U^∞	(1.4 ± 9.9)×10^{-5}	(9 ± 46)×10^{-7}	bar^{-1}
E_U	45 ± 19	59 ± 13	kJ/mol
b_H^∞	(6 ± 25)×10^{-4}	(5 ± 27)×10^{-4}	mol/(kg bar)
E_H	18 ± 11	18 ± 13	kJ/mol
χ_1	0.183 ± 0.069	0.124 ± 0.050	–
χ_2	(-9 ± 15)×10^2	0	K^{-1}
γ	4	4	–

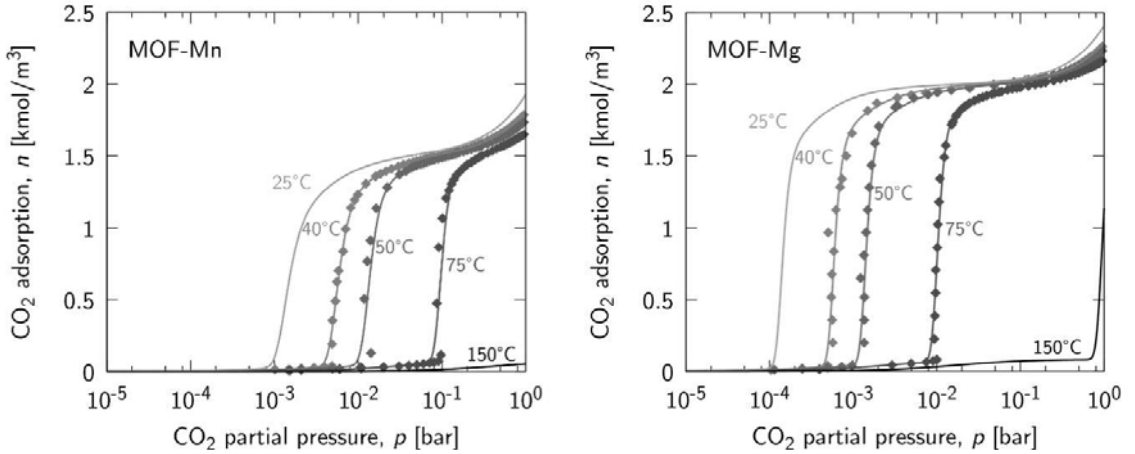

Fig. 3 CO_2 adsorption equilibrium measurement [3] and fitted w-DSL isotherm for MOF-Mn and MOF-Mg. Five isotherms (25°C, 40°C, 50°C, 75°C and150°C) are shown for both materials [4]. The mass specific adsorbed amount was converted to a volume specific quantity by multiplying with the bed density.

3.2. Assessment of the process performance

A fair comparison between processes must be carried out for a specific separation task and under optimal operating conditions. Before optimizing the specific energy consumption and the productivity of the process, it is necessary to assess their feasibility in delivering the specified separation task, i.e., a CO_2 recovery of over 90% in a 96% pure CO_2 product. Therefore, the operating conditions were first optimized to maximize both purity and recovery. The results are presented in Fig. 4 as Pareto fronts that delimit the feasible region (lower left) from the infeasible region (upper right). While there exist operating conditions that allow the process operated with MOF-Mn to reach the desired specifications, this is not the case for the process operated with MOF-Mg. In fact, the fixed high temperature level of 420 K considered in this work is too low to desorb sufficient CO_2 from MOF-Mg.

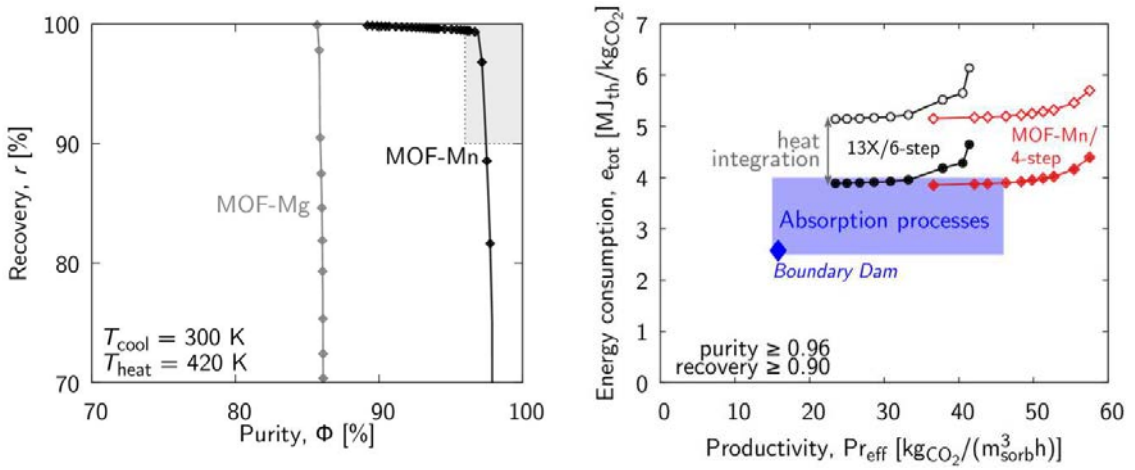

Fig. 4 Achievable recovery and purity for the considered TSA process with MOF-Mn and MOF-Mg (left) [4]. Productivity and energy consumption for operating conditions achieving CO2 purity ≥ 96% and CO2 recovery ≥ 90% for MOF-Mn as compared to a 6-step TSA process operated with zeolite 13X [8]. The empty and solid symbols correspond to the performance before and after applying heat integration according to Joss et al. [10], respectively.

Fig. 4 on the right shows the results of the optimized TSA process with MOF-Mn (empty diamonds). The optimal points form again a Pareto frontier, showing the trade-off between productivity and specific energy consumption. The performance of the MOF-Mn material with the 4-step cycle is compared to the state-of-the-art TSA process, i.e., a 6-step cycle operated with a commercial zeolite 13X [11]. It is interesting to note that the specific energy consumption is very similar between both processes. On the other hand, as compared to the zeolite 13X, MOF-Mn achieves higher productivity while using a simpler process.

4. Discussion and conclusions

The range of performance representative of state-of-the-art amine scrubbing processes (Boundary Dam [12], NETL [13], IEAGHG [14]) is indicated by a blue rectangle in Fig. 4. As compared to amine scrubbing technologies, TSA processes still come with a larger energy penalty. However, it is imported to point out that TSA does not have the same level of maturity as amine scrubbing, and there still exist several opportunities for improvement. Of particular interest is the possibility of designing an efficient heat integration strategy. The solid symbols shown in Fig. 4 correspond to the performance of both the 4-step/MOF-Mn and the 6-step/13X TSA processes when heat integration calculations as described by Joss et al. [11] are considered, i.e., heat recovery from a low grade heat source, such as the hot flue gas itself, and internal heat integration between heating and cooling steps of the TSA process. When applying heat integration, TSA processes show similar performance as compared to amine-scrubbing processes.

The results reported here and in other recent works [4,9,11] highlight the feasibility of TSA for post-combustion CO_2 capture and motivates future work aimed at improving adsorbent materials, process design and all other engineering aspects related to these processes, such as material formulation, engineering of column modules and system integration and optimization.

References

[1] Caskey SR, Wong-Foy AG, Matzger AJ. Dramatic tuning of carbon dioxide uptake via metal substitution in a coordination polymer with cylindrical pores. J Am Soc 2008; 130:48109–55.

[2] Coudert FX, Boutin A, Fuchs AH, Neimark A. Adsorption deformation and structural transitions in metal-organic frameworks: From the unit cell to the crystal. J Phys Chem Lett 2013; 4:3198–205.

[3] McDonald TM, et al. Cooperative insertion of CO2 in diamine-appended metal-organic frameworks. Nature 2015; 519:303–8.
[4] Hefti M, Joss L, Bjelobrk Z, Mazzotti M. On the potential of phase change adsorbents for CO_2 capture by temperature swing adsorption. Faraday Discuss 2016; 10.1039/C6FD00040A.
[5] Mason JA et al. Application of a High-Throughput Analyzer in Evaluating Solid Adsorbents for Post-Combustion Carbon Capture via Multicomponent Adsorption of CO_2, N_2 and H_2O. J Am Soc 2015: 137:4787–803.
[6] Smith RC. Uncertainty quantification: Theory, Implementation, and Applications. SIAM, 2014.
[7] Mersmann A. Ullmann's Encyclopedia of Industrial Chemistry. VCH Publishers Inc, Weinheim, 5th edn, 1988, ch. Adsorption.
[8] Casas N, Schell J Joss L, Mazzotti M. A parametric study of a PSA process for pre-combustion CO_2 capture. Sep Purif Technol 2013; 104:183–92.
[9] Marx D, Joss L, Hefti M, Mazzotti M. Temperature swing adsorption for postcombustion CO_2 capture: Single and multicolumn experiments and simulations. Ind Eng Chem Res 2016; 55:1401–12.
[10] Joss L, Capra F, Gazzani M, Mazzotti M, Martelli E. MO-MCS: An efficient multi-objective optimization algorithm for the optimization of temperature/pressure swing adsorption cycles. Comp Aided Chem Eng 2016; 38:1467–72.
[11] Joss L, Gazzani M, Mazzotti M. Rational design of temperature swing adsorption cycles for post-combustion CO_2 capture. Chem Eng Sci 2016; under review.
[12] Couturier G. SaskPower Boundary Dam carbon capture demonstration project. 2014; http://wyia.org/documents/presentations/presentations-wias-winter-board-meeting-cheyenne-wy-january-23-24-2014/
[13] Ramezan M, Skone TJ Nskala YN Lilijedahl G. Carbon dioxide capture from existing power plants. NETL Report 2007.
[14] IEAGHG, Incorporating future technologiecal improvements in existing CO_2 post combustion capture plants: Technical review. 2013/TR5 May 2013.